JOINT INSTITUTE FOR ADVANCEMENT OF FLIGHT SCIENCES

FINAL REPORT

NAG1-573

School of Engineering and Applied Science
The George Washington University
Washington, D. C. 20052

Numerical Simulation of Separated Flows over Arbitrary Airfoils and Their Resulting Wakes

Introduction

The aerodynamic design of a flight vehicle must carefully account for the drag. The estimation of the drag is greatly affected by viscous effects. For flows of practical interest, the Reynolds number is sufficiently large for the flow field to be divided into viscous and inviscid zones, e.g., the problem of flow past wing. Different approaches are available for solving such a problem. Inherently, the Navier-Stokes formulations lead to an extremely stiff nonlinear system. Using an explicit algorithm to solve such problems results in the requirement of very small time-steps in order to satisfy the stability bounds. Therefore, many iterations and large computer times are required to reach the steady-state. To remove the time-step restriction, fully implicit methods have been investigated. The implicit methods, however, still require many iterations to reach the steady state and consequently, still require large computational costs.

In an effort to decrease the computational costs associated with the implicit algorithms, many different procedures have been studied, in particular the Pulliam-Chaussee diagonalization procedure[1] and the Barth-Steger matrix reduction method.[2] New dissipation models[3] and spatially varying time-steps have dramatically increased the convergence rate. However, one problem still remains: long running times for general configuration. In aircraft design, any pertinent parameters must be accurately predicted (C_L, C_D, etc.). To this end, high resolution is required in order to accurately compute the flow physics of shock and boundary-layer interaction, massive separation and turbulent flow structures.

To overcome the problem of grid generation for complicated geometries and long tunning times, zonal approaches have become increasingly popular. By

zonal approach we mean partitioning of the flow field into distinct zones each of which is solved independently, where the length scales associated with each individual region are honored. There are a number of advantages for the zonal technique. First, the difficulty in generating three-dimensional grids for different types of complex configurations can be eliminated with the use of zonal methods. Second, zonal methods would allow different types of grid topologies to be implemented where appropriate in order for the grids to be mesh-efficient, that is, more points on the configuration, where accuracy is desired, and fewer points in the outer flow field. And finally, finer meshes can be used in those regions of rapid changes in the flow quantities, for example, in the regions where shocks occur, in the viscous boundary layer, or where vorticity is generated. The zonal concept has been successfully applied by the author[4,5,6] to some model problems for two-dimensional and axisymmetric flows.

The present work is a generalization and improvement of an earlier work developed for studying separated flows using boundary layer type equations. The improvements include extensions to a general coordinate system and use of a more general zonal technique for solving the coupled equations. In order to be able to consider arbitrary geometries, second order accurate (in space) conservative differences are generated by considering the integral formulation of the governing equations in a general coordinate system. The general coordinate system is handled in as general a manner as possible to allow for the use of either analytically or numerically generated coordinate systems.

The present work used a marching procedure for solving the PPNS (Partially Parabolized Navier-Stokes) equations in the viscous region coupled in a fully implicit manner with the elliptic inviscid equation. To test the algorithm and compare to other solutions, solutions for flow over a flat plate and

flow past the symmetrical 12-percent-thick Joukowski airfoil (J012) at zero angle of attack were obtained.

Analysis

The basic equations which describe the motion of laminar incompressible flow are the Navier-Stokes equations. These equations can be written in stream function-vorticity (ψ-ω) form in general coordinates,

$$-J\omega = \frac{\partial}{\partial \xi}\left(\frac{\alpha}{J}\frac{\partial \psi}{\partial \xi} - \frac{\beta}{J}\frac{\partial \psi}{\partial \eta}\right) + \frac{\partial}{\partial \eta}\left(\frac{\alpha}{J}\frac{\partial \psi}{\partial \eta} - \frac{\beta}{J}\frac{\partial \psi}{\partial \xi}\right) \tag{1}$$

and

$$J\frac{\partial \omega}{\partial t} + \frac{\partial \psi}{\partial \eta}\frac{\partial \omega}{\partial \xi} - \frac{\partial \psi}{\partial \xi}\frac{\partial \omega}{\partial \eta} = \frac{1}{R_e}\left\{\frac{\partial}{\partial \xi}\left(\frac{\alpha}{J}\frac{\partial \omega}{\partial \xi} - \frac{\beta}{J}\frac{\partial \omega}{\partial \eta}\right) + \frac{\partial}{\partial \eta}\left(\frac{\alpha}{J}\frac{\partial \omega}{\partial \eta} - \frac{\beta}{J}\frac{\partial \omega}{\partial \xi}\right)\right\} \tag{2}$$

where

$$\alpha = x_\eta^2 + y_\eta^2 \tag{3}$$

$$\beta = x_\xi x_\eta + y_\xi y_\eta \tag{4}$$

$$\alpha = x_\xi^2 + y_\xi^2 \tag{5}$$

$$J = x_\xi y_\eta - x_\eta y_\xi \tag{6}$$

and R_e is the Reynolds number.

If the chosen coordinate system is orthogonal, then β is zero.

Defining the unit vectors in the (ξ,η) coordinate system as $(\vec{e}_1,\vec{e}_2)$, the velocity vector $\vec{V}$ can be expressed as

$$\vec{V} = u\vec{e}_1 + v\vec{e}_2 \tag{7}$$

where u and v are the components of $\vec{V}$ defined as,

$$u = \frac{\partial \psi}{\partial \eta} \tag{8}$$

$$v = -\frac{\partial \psi}{\partial \xi} \tag{9}$$

The relation between the Cartesian velocity components (u_c, v_c) and the present velocity components (u,v) is,

$$u_c = \frac{x_\xi u + x_\eta v}{J} \tag{10}$$

$$v_c = \frac{y_\xi u + y_\eta v}{J} \tag{11}$$

Evaluation of the Pressure

The momentum equations can be written as

$$\rho \vec{V} \cdot \nabla \vec{V} = -\nabla P - \mu \nabla^2 \vec{V} \tag{12}$$

where p is the pressure and ρ is the density.

Multiplying the x-momentum equation by dx and the y-momentum equation by dy and adding the two to get a single equation for the pressure,

$$\rho \frac{\partial}{\partial x}\left(\frac{u_c^2 + v_c^2}{2}\right)dx + \rho \frac{\partial}{\partial y}\left(\frac{u_c^2 + v_c^2}{2}\right)dy - \rho v_c \frac{\partial v_c}{\partial x}\,dx - \rho u_c \frac{\partial u_c}{\partial y}$$

$$+ \rho u_c \frac{\partial v_c}{\partial x}\,dy + \rho v_c \frac{\partial u_c}{\partial y}\,dx = -\left(\frac{\partial P}{\partial x}\,dx + \frac{\partial P}{\partial y}\,dy\right) + \mu\left(\frac{\partial \omega}{\partial x}\,dy - \frac{\partial \omega}{\partial y}\,dx\right) \tag{13}$$

Equation (13) can be written as,

$$d[\rho \frac{V^2}{2} + P] + \rho\omega \, d\psi = \mu(\frac{\partial \omega}{\partial x} dy - \frac{\partial \omega}{\partial y} dx) \tag{14}$$

The Cartesian operators can be expresed in terms of the general coordinates as

$$\frac{\partial}{\partial x} = \frac{1}{J} (y_\eta \frac{\partial}{\partial \xi} - y_\xi \frac{\partial}{\partial \eta}) \tag{15}$$

and

$$\frac{\partial}{\partial y} = \frac{1}{J} (x_\xi \frac{\partial}{\partial \eta} - x_\eta \frac{\partial}{\partial \xi}) \tag{16}$$

Equation (13) is expressed in terms of the general coordinates as,

$$d[\rho \frac{V^2}{2} + P] = -\rho\omega d\psi + \mu[\frac{\beta}{J} \frac{\partial \omega}{\partial \xi} - \frac{\alpha}{J} \frac{\partial \omega}{\partial \eta}] d\xi + \mu[-\frac{\beta}{J} \frac{\partial \omega}{\partial \eta} + \frac{\alpha}{J} \frac{\partial \omega}{\partial \xi}] d\eta \tag{17}$$

Or in terms of C_p (pressure coefficient),

$$d[V^2 + C_p] = -2\omega d\psi + \frac{2}{R_e} \{(\frac{\beta}{J} \omega_\xi - \frac{\alpha}{J} \omega_\eta) d\xi + (-\frac{\beta}{J} \frac{\partial \omega}{\partial \eta} + \frac{\alpha}{J} \frac{\partial \omega}{\partial \xi}) d\eta\} \tag{18}$$

Inviscid Analysis

The inviscid solution in the present work is obtained from an incompressible stream function representation of the inviscid flow region with zero vorticity. The boundary conditions for the inviscid region are, at the inflow boundary, $\xi=\xi_1$, $u=u_\infty$. On the interface ψ is known from the coupling between the viscous and inviscid zones, and for $\eta \to \infty$, $u \to u_\infty$. At the outer flow boundary, $\xi=\xi_0$, $\psi_x = 0$ (see reference 6 for more details).

A second order accurate conservative difference scheme is generated for the stream function equation, by integrating the equation around a differential

element in the physical domain. The resulting algebraic system of equations is solved iteratively with the SLOR (Successive Line Over Relaxation) scheme. At each ξ-line in the computational domain, the finite difference equation at each nodal point is

$$a_J \delta\psi_{J-1} + b_J \delta\psi_J + c_J \delta\psi_{J+1} = d_J \tag{19}$$

where the index J denotes the grid position in the η direction and $\delta\psi$ the change of ψ between successive iterations, that is

$$\delta\psi = \psi^{n+1} - \psi^n \tag{20}$$

Along each ξ-line, a tridiagonal system of equations is solved using the Thomas algorithm.

Viscous Analysis

The flow in the viscous region is assumed to be governed by PPNS or (TL) equations,

$$\frac{\partial}{\partial \xi}(\omega\psi_\eta) - \frac{\partial}{\partial \eta}(\omega\psi_\xi) = \frac{1}{R_e}\frac{\partial}{\partial \eta}\left(\frac{\alpha}{J}\frac{\partial \omega}{\partial \eta}\right) \tag{21}$$

and

$$J\omega + \frac{\partial}{\partial \xi}\left(\frac{\alpha}{J}\frac{\partial \psi}{\partial \xi} - \frac{\beta}{J}\frac{\partial \psi}{\partial \eta}\right) + \frac{\partial}{\partial \xi}\left(\frac{\alpha}{J}\frac{\partial \omega}{\partial \eta} - \frac{\beta}{J}\frac{\partial \psi}{\partial \xi}\right) \tag{22}$$

The above equations are to be solved in the viscous region.

Boundary conditions for the viscous equations are at the surface,

$$\eta = 0, \quad \psi = \psi_\eta = 0 \tag{23a}$$

at the interface,

$$\eta = \eta_{IN},\ \psi = \psi_{IN} \text{ (obtained from the coupling)},\ \omega = 0 \qquad (23b)$$

at the inflow boundary,

$$\xi = \xi_1,\ \psi = \psi(\eta),\ \omega = \omega\ (\eta) \qquad (23c)$$

at the outflow boundary,

$\xi = \xi_0$, viscid/inviscid interaction is negligible.

Central finite difference approximations are used everywhere except for the term $(\psi_\eta \delta\omega_\xi)$, which is treated as an upwind difference. That means, in the limit of the steady state, a second order accurate solution is obtained.

At each S line, the correction equations based on a Newton linearization procedure have the general form:

$$A\,\delta\psi_{I,J-1} + B\,\delta\psi_{I,J} + C\,\delta\psi_{I,J+1} + D\,\delta\omega_{I,J-1} + E\,\delta\omega_{I,J} + F\,\delta\omega_{I,J+1} = R_1 \qquad (24a)$$

$$a\,\delta\psi_{I,J-1} + b\,\delta\psi_{I,J} + c\,\delta\psi_{I,J+1} + d\,\delta\omega_{I,J-1} + e\,\delta\omega_{I,J} + f\,\delta\omega_{I,J+1} = R_2 \qquad (24b)$$

A block (2x2) tridiagonal Thomas algorithm is used, where in the forward pass, the coefficients are calculated starting with the interface boundary conditions. The boundary condition at the surface and the coupling between viscous and inviscid zones are treated between viscous and inviscid zones are treated in the same way described in reference 6.

Numerical Generation of Metric Coefficients

As explained, one way of generating a second order accurate conservative differencing scheme includes calculating the metric coefficients and the Jacobian of the coordinate transformation at the center (in the transformed plane) of each side of the differential element shown in sketch 1.

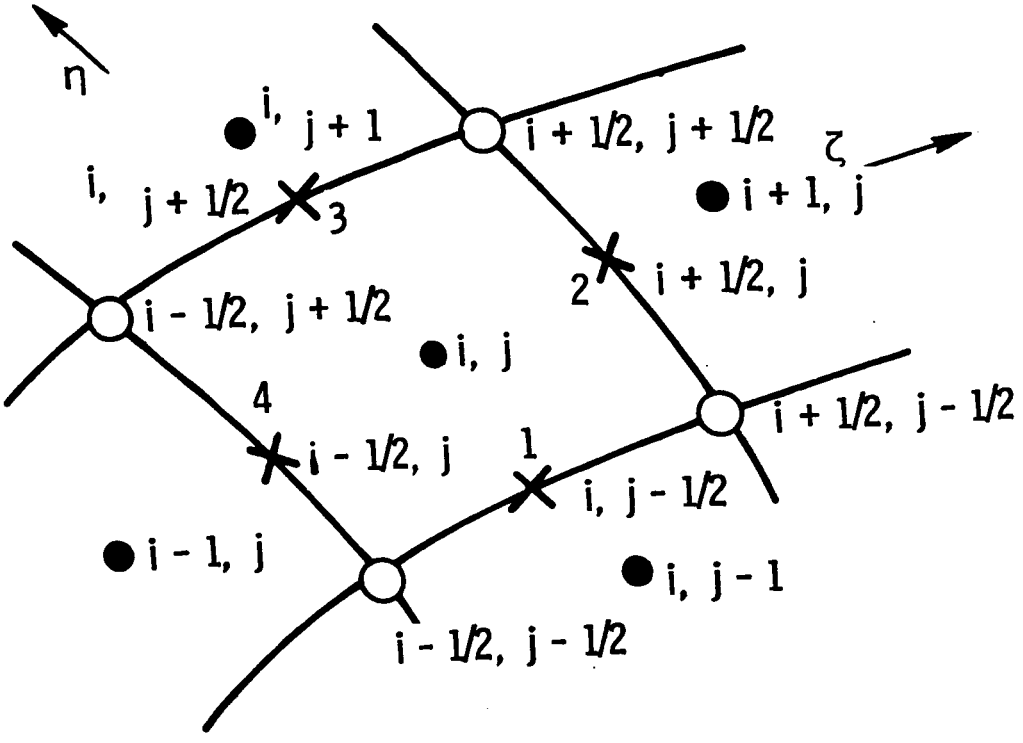

Sketch 1, Differential Element

On sides 1 and 3 the coefficients $\frac{\alpha}{J}$ and $\frac{\beta}{J}$ will be calculated while $\frac{\alpha}{J}$ and $\frac{\beta}{J}$ will be calculated on sides 2 and 4. Using side 1 as an example, α_1, β_1 and J_1 were previously defined as,

$$\alpha_1 = x_{1\xi}^2 + y_{1\xi}^2 \tag{25}$$

$$\beta_1 = x_{1\xi}\, x_{1\eta} + y_{1\xi}\, y_{1\eta} \tag{26}$$

and

$$J_1 = x_{1\xi}\, y_{1\eta} - x_{1\eta}\, y_{1\xi} \tag{27}$$

Along side 1, $\Delta\eta = 0$, therefore,

$$\Delta x_1 = x_{1\xi}\, \Delta\xi_1 \tag{28}$$

or

$$x_{1\xi} = \frac{\Delta x_1}{\Delta\xi_1} \tag{29}$$

Using the subscripts in sketch 1,

$$x_{1\xi_{i,j-1/2}} = \frac{x_{i+1/2,\,j-1/2} - x_{i-1/2,\,j-1/2}}{\Delta\xi} \tag{30}$$

where $\Delta\xi_1 = \Delta\xi_3 = \Delta\xi$ = constant.

Similarly,

$$y_{1\xi_{i,j-1/2}} = \frac{y_{i+1/2,\,j-1/2} - y_{i-1/2,\,j-1/2}}{\Delta\xi}$$

These central differences are second order accurate in space. Therefore, α_1 can be represented to second order accuracy as

$$\alpha_1 = \alpha_{i,j-1/2} = (x_{1\xi_{i,j-1/2}})^2 + (y_{1\xi_{i,j-1/2}})^2 \tag{31}$$

The coefficients β and J include the terms $x_{1\eta}$ and $y_{1\eta}$. $x_{1\eta}$ and $y_{1\eta}$ are calculated in the same manner as $x_{1\xi}$ and $y_{1\eta}$, and their second order accurate finite difference representations are

$$x_{1\eta_{i,j-1/2}} = \frac{x_{i,j} - x_{i,j-1}}{\Delta\eta} \tag{32}$$

$$y_{1\eta_{i,j-1/2}} = \frac{y_{i,j} - y_{i,j-1}}{\Delta\eta} \tag{33}$$

Therefore, the second order accurate representations of β_1 and J_1 are

$$\beta_1 = \beta_{i,j-1/2} = (x_{1\xi_{i,j-1/2}})(x_{1\eta_{i,j-1/2}}) + (y_{1\xi_{i,j-1/2}})(y_{1\eta_{i,j-1/2}}) \tag{34}$$

and

$$J_1 = J_{i,j-1/2} = (x_{1\xi_{i,j-1/2}})(y_{1\eta_{i,j-1/2}}) - (x_{1\eta_{i,j-1/2}})(y_{1\xi_{i,j-1/2}}) \tag{35}$$

The finite difference expressions for the metric coefficients and Jacobian of the transformation at the center of the remaining element sides are derived analogously. Therefore, to generate the metric coefficients and Jacobians throughout the solution plane with central differences, the Cartesian coordinates of the algorithm solution points, the corners of the differential elements, and the points outside the boundaries, must be known.

Results and Discussion

The algorithm was tested for two cases. The first case was flow over a flat plate and the second one was flow past the symmetrical Joukowski airfoil J012 at zero angle of attack. The flat plate solution exactly matched the known Blasius solution. For the case of J012 airfoil, the choice of the grid is very critical for viscous computations over airfoils. There has been general agreement that C type grids are the best for handling the trailing edge and wakes for airfoils. One clear advantage of the present formulation is the complete independence on the way by which the grid is generated. That means the present scheme is capable of solving any type of grids. A C type grid for J012 airfoil used by NASA Langley, see figure 1, was implemented for the present work. Only half of the grid (Figure 2) was used for the actual

computations due to the symmetry of the problem. The grid shown in Figure 1 is a coarse grid for high Reynolds number flows. Only two Reynolds number solutions (R_e=1000 and R_e=2000) were obtained for the grid shown in figure 2. Figure 3 shows the friction coefficient ($\bar{c}_f$) over the surface of the airfoil at R_e=1000. The value of $\bar{c}_f$ in the vicinity of the leading edge of the airfoil is in complete agreement with the stagnation point flow[8] solution ($\phi_{\eta\eta_w}$=1.2326). The values of $\bar{c}_f$ near the trailing edge of the airfoil were magnified on a larger scale to be able to see the solution in that region (Figure 4). As the R_e increased up to 2000, the flow separated at 64% of the chord in accordance of the experimental data of reference 8, and the solution of the integral form of the boundary layer equations, see figure 5. The values of $\bar{c}_f$ in the separated region are displayed on a larger scale, figure 6. The streamline contours are given in figure 7.

Conclusion

The contribution of the current work lies in the generalization of the zonal technique for solving separated flows over any arbitrary airfoil. A numerical study of the aerodynamic characteristics for airfoils near stall is viable using the developed method.

Acknowledgment

The present work and the work reported in reference 6 was supported by NASA Langley Grant NAG1-573. The discussion with J. Thomas and C. Rumsey of the Analytical Methods Branch is appreciated.

References

1. Pulliam, T. H. and Chaussee, D. S., "A Diagonal Form of an Implicit Approximate-Factorization Algorithm," Journal of Computational Physics, Vol. 22, 1976, pp. 87-110.

2. Barth, T. and Steger, J. L., "A Fast Efficient Implicit Scheme for the Gasdynamic Equations Using Matrix Reduction Technique," AIAA Paper No. 85-0439, Reno, Nevada, 1985.

3. Pulliam, T. H., "Artificial Dissipation Models for the Euler Equations," AIAA Paper No. 85-0438, Reno, Nevada, 1985.

4. Halim, A., and Hafez, M., "Calculation of Separation Bubbles Using Boundary Layer-Type Equations, Part I," Chapter in Recent Advances in Numerical Methods in Fluids, Vol. 3, pp. 395-415, Pineridge Press Limited, Swansea, United Kingdom, 1984.

5. Halim, A., and Hafez, M., "Calculation of Separation Bubbles Using Boundary Layer-Type Equations/Part II," AIAA J., April 1986. Also AIAA Paper 84-1585, Snowmass, Colorado, 1984.

6. Halim, A., "Development of a Boundary-Layer-Type Solver Based on Simultaneous Iteration Technique for Axisymmetric Separated Flows," AIAA CP 854, pp. 150-161; AIAA Paper No. 85-1505.

7. Thomas, J. and Rumsey, C., NASA Langley, Private Communication.

8. Schlichting, H., Boundary Layer Theory, McGraw-Hill Book Company.

9. Bussmann, K. and Ulrich, A., "Systematic Investigation of the Influence of the Shape of the Profile upon the Position of the Transition Point," NACA TM-1185, 1943.

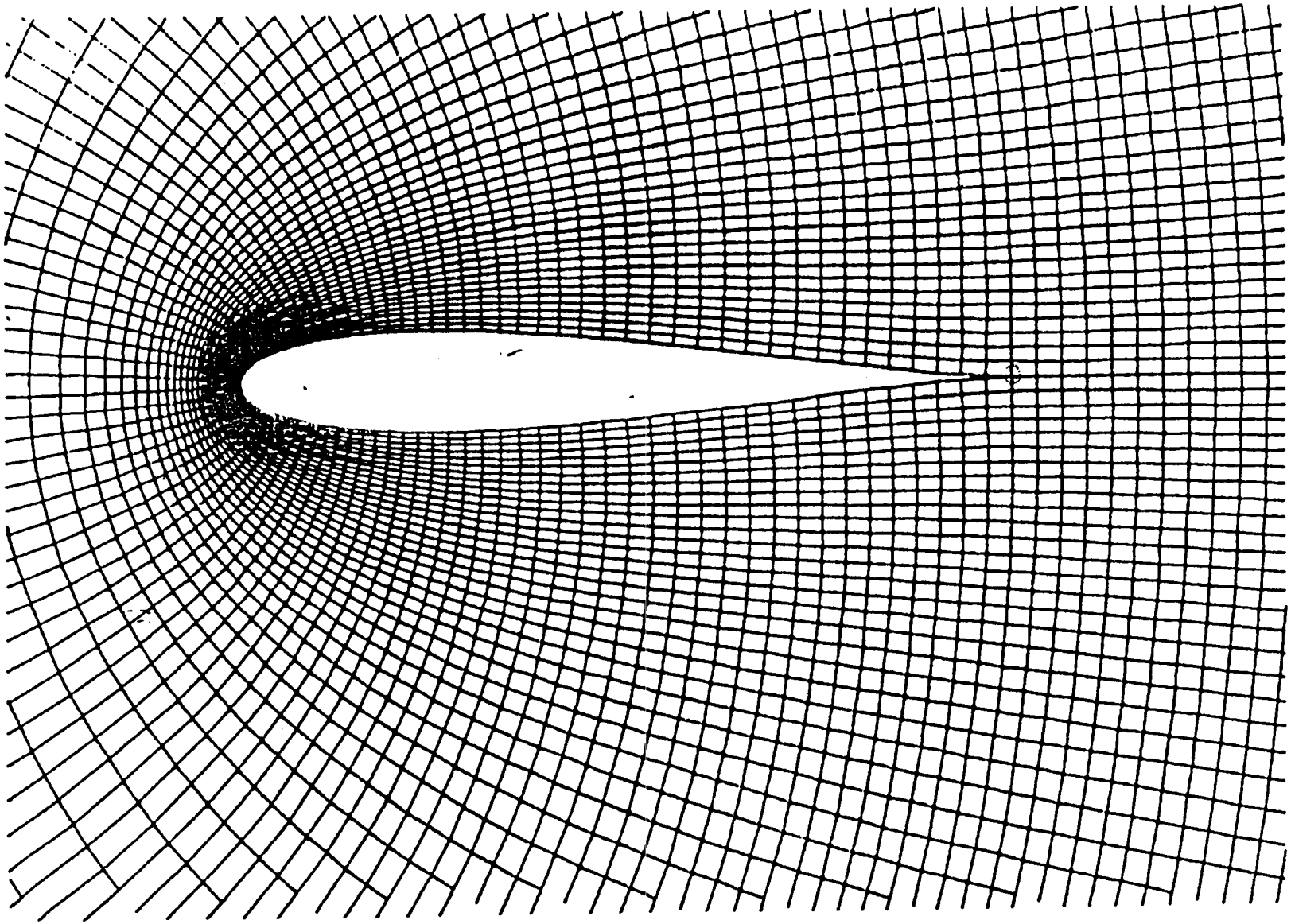

FIGURE 1. C TYPE GRID FOR J012 AIRFOIL

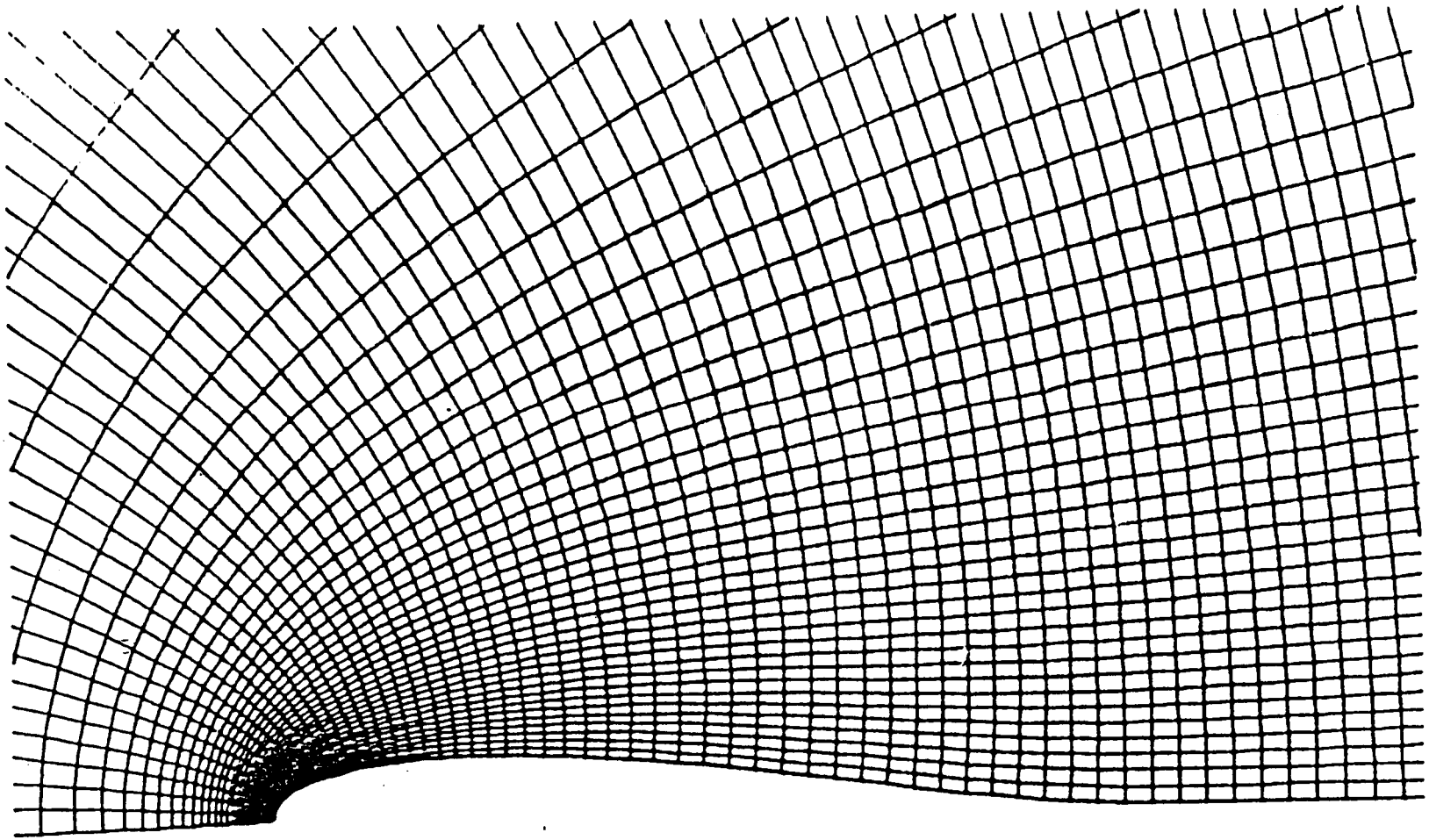

FIGURE 2. HALF OF THE GRID USED FOR ACTUAL COMPUTATIONS

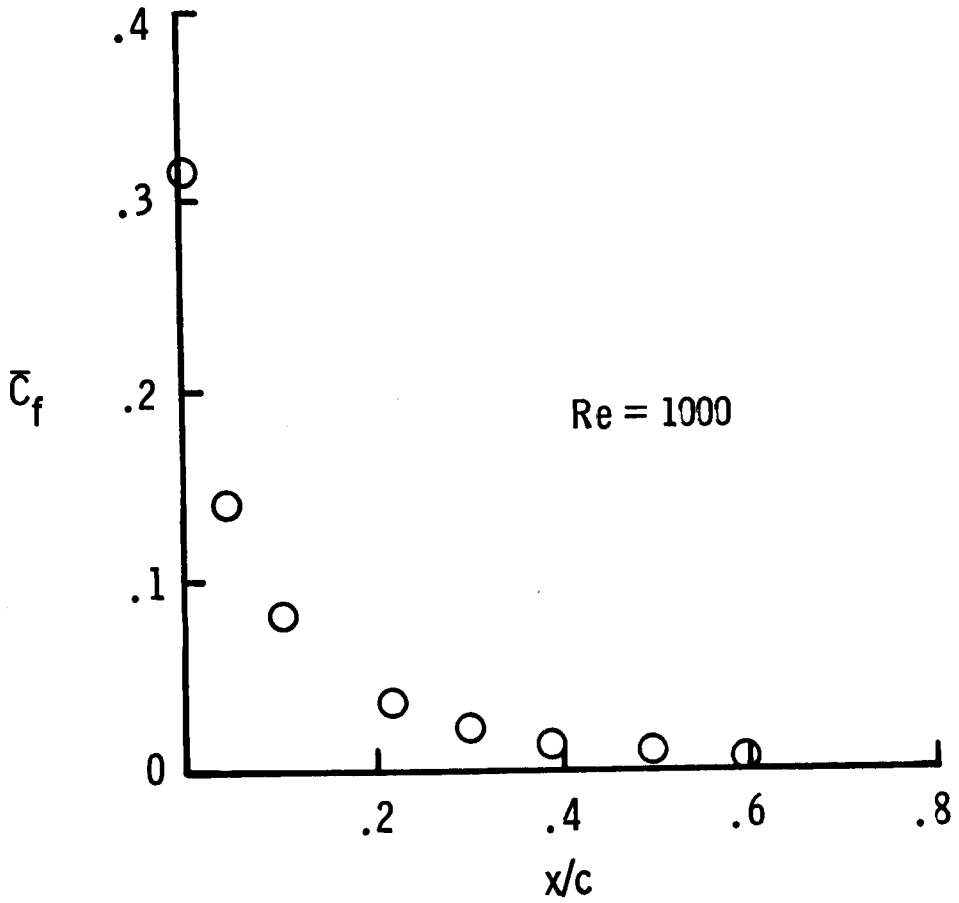

Figure 3. Shear Stress Distribution Over the J012 Airfoil

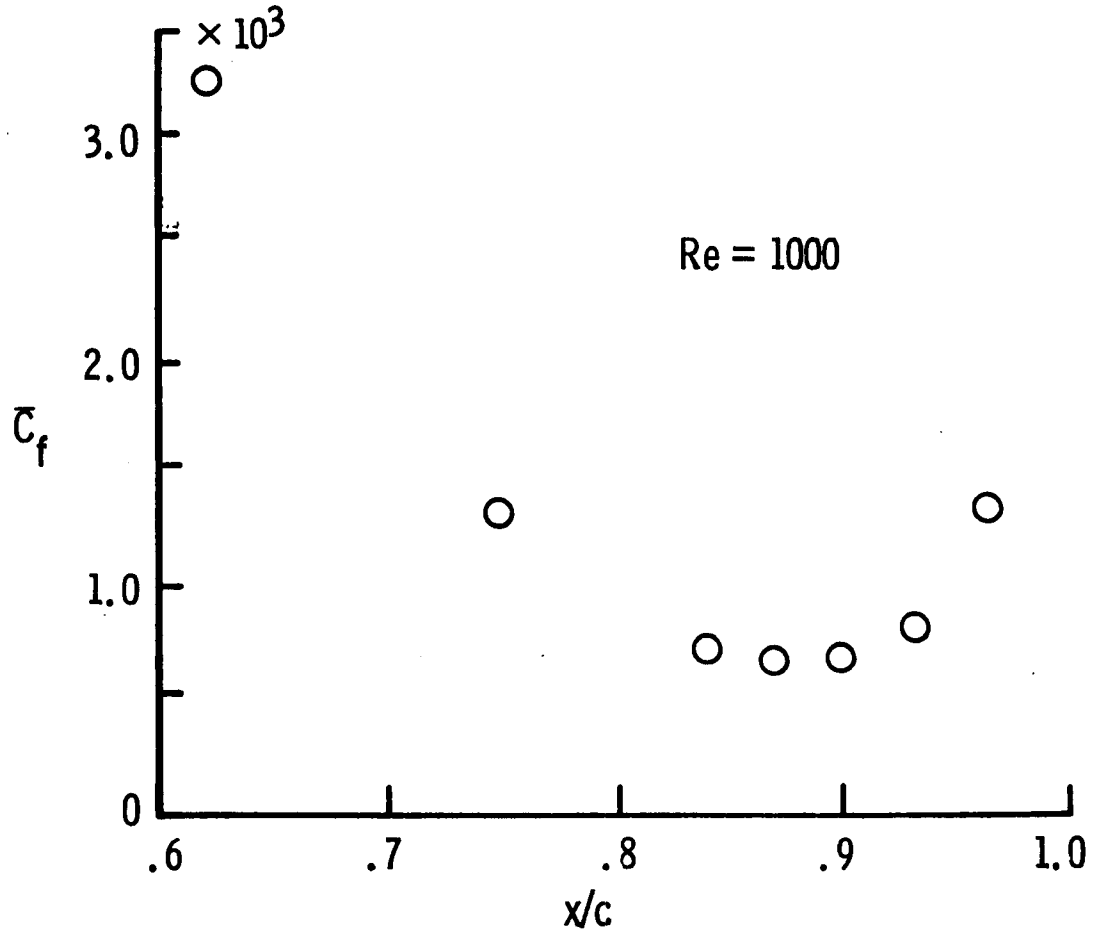

Figure 4. Detailed Study of Shear Stress Near T.E.

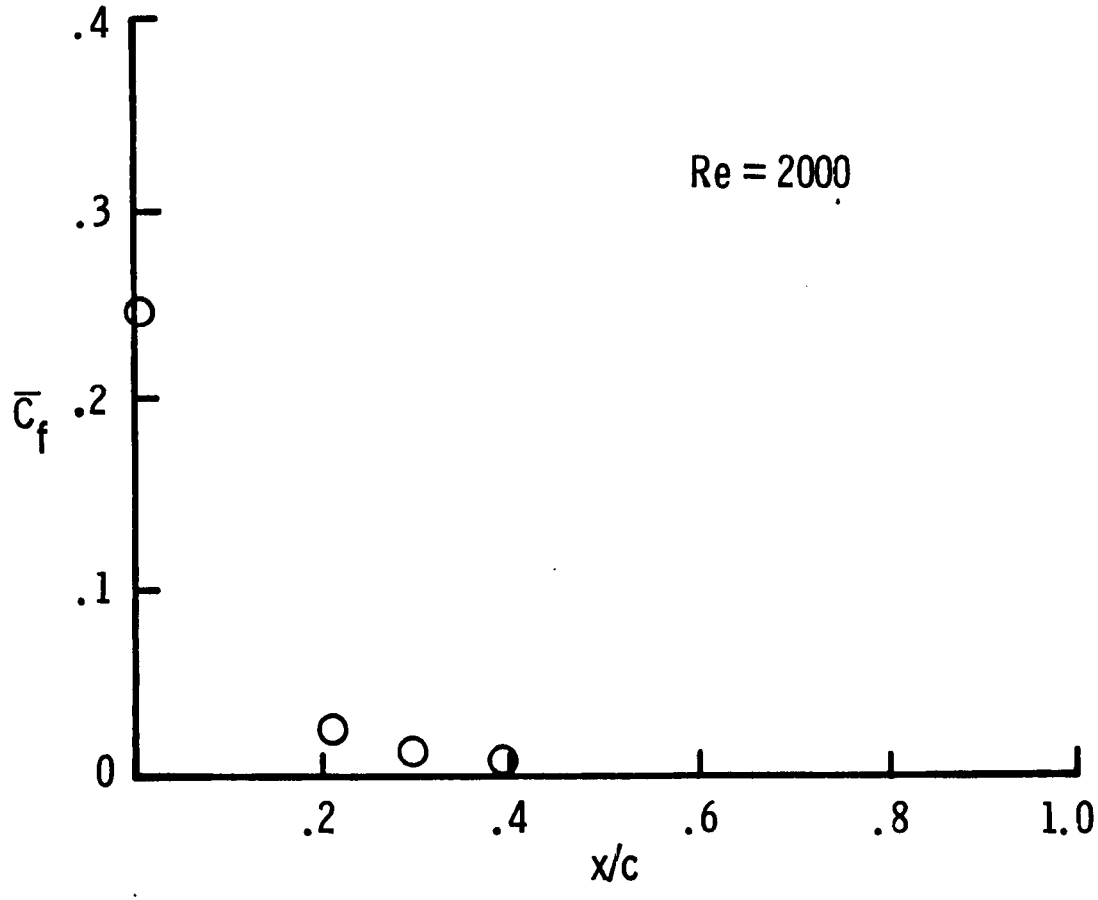

Figure 5. Shear Stress Distribution Over the J012 Airfoil. Re = 2000

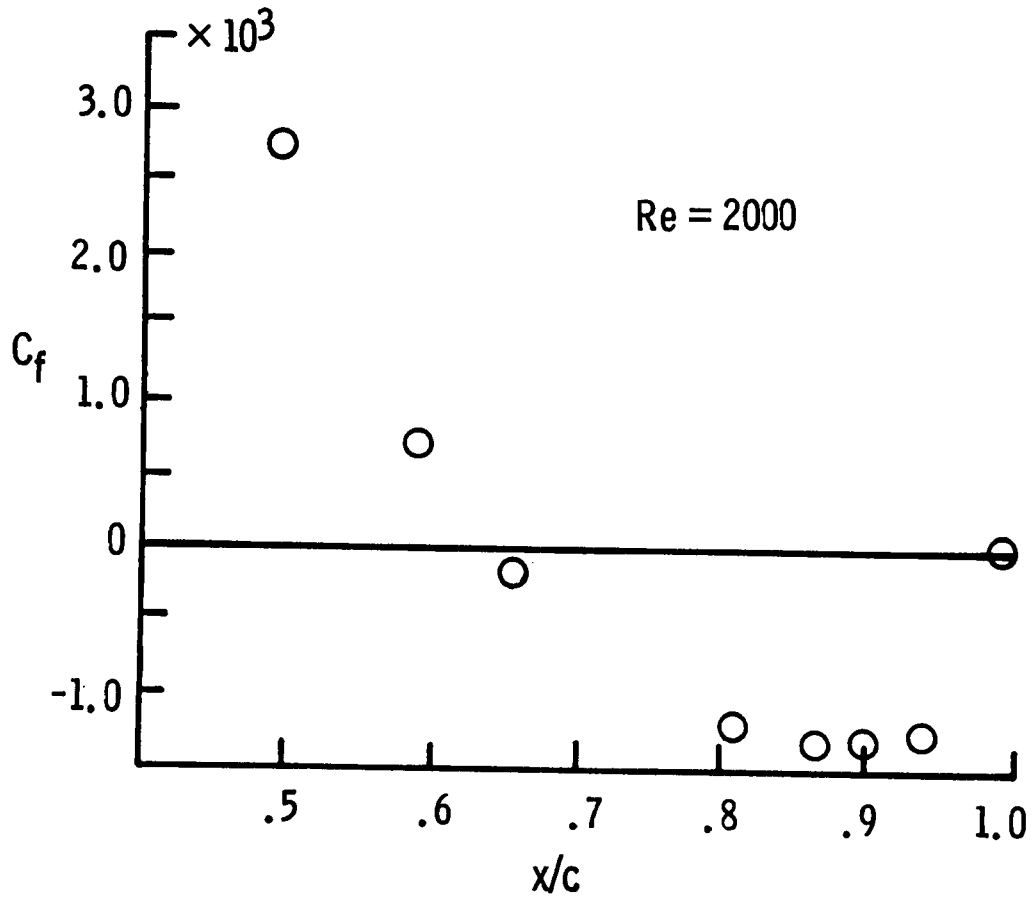

Figure 6. Detailed Study of Shear Stress in the Separated Region

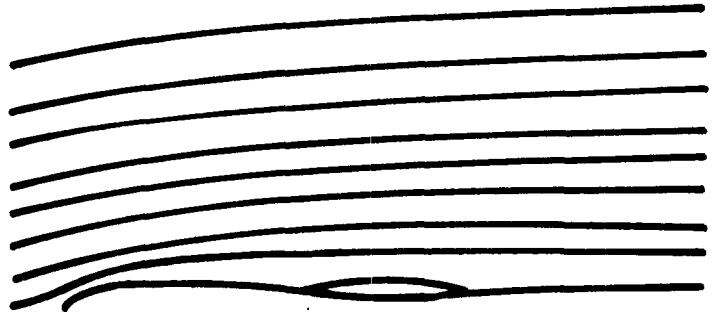

Figure 7. Streamline Contours for Flow Over J012 Airfoil.
Re = 2000